

# Trajectory Imputation in Multi-Agent Sports with Derivative-Accumulating Self-Ensemble

Han-Jun Choi<sup>1\*</sup> Hyunsung Kim<sup>2,3\*</sup>, Minho Lee<sup>4</sup>, Minchul Jeong<sup>5</sup>,  
Changjo Kim<sup>3</sup>, Jinsung Yoon<sup>3</sup>, and Sang-Ki Ko<sup>6</sup>

<sup>1</sup> KETI, Seongnam, South Korea  
hanjun\_c@keti.re.kr

<sup>2</sup> KAIST, Daejeon, South Korea  
hyunsung.kim@kaist.ac.kr

<sup>3</sup> Fitotogether Inc., Seoul, South Korea  
{hyunsung.kim, changjo.kim, jinsung.yoon}@fitotogether.com

<sup>4</sup> Saarland University, Saarbrücken, Germany  
minho.lee@uni-saarland.de

<sup>5</sup> Weflo Inc., Seoul, South Korea  
mcjeong@weflo.ai

<sup>6</sup> University of Seoul, Seoul, South Korea  
sangkiko@uos.ac.kr

**Abstract.** Multi-agent trajectory data collected from domains such as team sports often suffer from missing values due to various factors. While many imputation methods have been proposed for spatiotemporal data, they are not well-suited for multi-agent sports scenarios where player movements are highly dynamic and inter-agent interactions continuously evolve. To address these challenges, we propose MIDAS (**M**ulti-agent **I**mputer with **D**erivative-**A**ccumulating **S**elf-ensemble), a framework that imputes multi-agent trajectories with high accuracy and physical plausibility. It jointly predicts positions, velocities, and accelerations through a Set Transformer-based neural network and generates alternative estimates by recursively accumulating predicted velocity and acceleration values. These predictions are then combined using a learnable weighted ensemble to produce a final imputed trajectories. Experiments on three sports datasets demonstrate that MIDAS significantly outperforms existing baselines in both positional accuracy and physical plausibility. Lastly, we showcase use cases of MIDAS, such as approximating total distance and pass success probability, to highlight its applicability to practical downstream tasks that require complete tracking data.

**Keywords:** Sports Analytics · Multi-Agent System · Trajectory Imputation · Deep Learning under Physical Constraints · Weighted Ensemble

## 1 Introduction

Many spatiotemporal domains such as transportation, robotics, surveillance, and sports handle multi-agent trajectory data. Although advances in computer vision

---

\* These authors contributed equally to the paper.

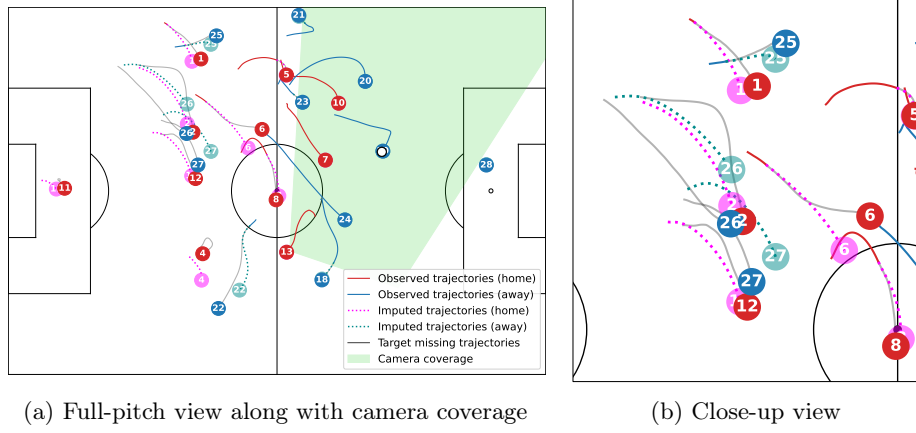


Fig. 1: Example of imputing unobserved player trajectories from tracking data obtained in a soccer broadcast.

and sensing technologies have facilitated large-scale trajectory data collection, acquiring complete trajectory data remains challenging due to various factors. Wearable devices such as GPS trackers and motion sensors may experience temporary signal loss or malfunction, and computer vision systems often miss agents due to occlusions or limitations of the camera’s field of view as instantiated in Fig. 1. This prevalence of missing values calls for the development of effective imputation techniques that can accurately reconstruct missing trajectories.

Though various imputation methods have been proposed for spatiotemporal data, applying them to multi-agent sports remains challenging due to their dynamic nature. In particular, while many of them [2,5,15,16,17,23] have demonstrated their effectiveness in multi-sensor data such as including traffic flow or air quality datasets, they did not account for dynamic interactions between agents. In such fixed-sensor networks, spatial relationships are typically static and the underlying system structure remains constant over time. In contrast, multi-agent domains such as team sports involve players whose positions are continuously changing, requiring suitable architecture for explicitly modeling these dynamic inter-agent relationships while maintaining permutation-equivariance with respect to the agents. Furthermore, player motion is subject to biomechanical constraints that impose physical limits on their speed, acceleration, and directional changes. Therefore, imputed trajectories need to be not only accurate in terms of position but also physically plausible. However, due to the inherent uncertainty in player motion, existing imputation models [3,18] even with dedicated architecture for multi-agent embedding tend to generate inaccurate or physically unrealistic trajectories, especially with limited training data or long missing intervals.

Addressing these challenges, this paper proposes MIDAS (**M**ulti-agent **I**mputer with **D**erivative-**A**ccumulating **S**elf-ensemble), a framework that imputes missing trajectories in multi-agent sports with high accuracy and physical plausibility

by enforcing the physical constraints that real player trajectories should satisfy. First, a neural network equipped with Set Transformers [12] and player-wise bidirectional LSTMs [9] predicts the positions, velocities, and accelerations of missing players. In addition to this *initial prediction* (IP), it generates alternative estimates through *derivative-accumulating prediction* (DAP), which recursively accumulates the predicted velocity and acceleration values from the nearest observed positions for each missing segment in both directions. Finally, the weighted soft voting mechanism combines these three types of prediction, i.e. the IP and the forward/backward DAPs, by dynamically determining the weight of each prediction to produce the final imputed trajectories.

The proposed MIDAS overcomes the aforementioned challenges in three aspects. First, by employing the Set Transformer, it models dynamic inter-agent relationships while ensuring permutation-equivariance of agents. Second, by jointly predicting position, velocity, and acceleration and enforcing the physical consistency between them, it ensures that the imputed trajectories are not only accurate in terms of position, but also plausible and smooth in terms of velocity and acceleration. Third, through a learnable weighted ensemble, MIDAS improves the accuracy of the final imputed trajectories by addressing the physical inconsistency of IP and the error compounding problem of DAP. Experiments conducted on the three sports datasets demonstrate that MIDAS consistently outperforms existing baselines in terms of both positional accuracy and physical plausibility of imputed trajectories by a large margin.

In short, the main contributions of this paper include:

1. A Set Transformer-based imputation model specifically designed for multi-agent domains, which alone outperforms most existing baselines in sports trajectory imputation tasks.
2. The MIDAS mechanism, which simultaneously ensures accurate prediction of position, velocity, acceleration, and their physical consistency, resulting in producing both accurate and physically plausible trajectories.
3. Extensive experiments conducted on three benchmark datasets: soccer, basketball, and American football, demonstrating the generalizability and interoperability of the framework across different sports and data providers.
4. Real-world use cases of MIDAS, including the approximation of physical (e.g., total distance covered) and contextual (e.g., pass success probability) metrics based on imputed trajectories.

## 2 Related Work

Numerous methods have been proposed for time series and spatiotemporal data imputation. Early models such as BRITS [2], GRU-D [4], and MRNN [26] relied on sequential recurrence, but suffered from compounding errors due to their dependence on previous predictions. Non-autoregressive frameworks such as NAOMI [15], CSDI [23], and SAITS [7] mitigated this issue by enabling parallel imputation across time steps, improving robustness and efficiency. More recently,

methods like TIDER [14] and TimesNet [24] were developed to capture the temporal patterns such as seasonality or local biases. Other recent approaches further leverage graph structures (GRIN [6], SPIN [16], and NRTSI [20]), information bottlenecks (TimeCIB [5]), or low-rank priors (ImputeFormer [17]) to enhance imputation performance. Although they perform well on static multi-sensor systems, they are not designed to handle dynamic interactions in multi-agent scenarios.

Meanwhile, several frameworks proposed dedicated architectures for multi-agent imputation to capture shifting spatial relationships in the domain. Notable examples include Graph Imputer [18] and TransPORTmer [3], which employ graph networks [1] and set attention [12], respectively, to model dynamic player interactions while ensuring permutation equivariance. Interaction modeling is widely studied in future trajectory forecasting [8,11,13,22,25,27], but existing methods are not directly applicable to missing trajectory imputation.

### 3 Proposed Framework

Our study about multi-agent trajectory imputation assumes a scenario where the missing time intervals of players could differ from one another. To elaborate, let the trajectories of  $K$  players be  $X_{1:T} = \{\mathbf{x}_{1:T}^k\}_{k=1}^K$ , where each player  $k$ 's input features  $\mathbf{x}_t^k$  at each time  $t$  consist of their  $(x, y)$  position  $\mathbf{p}_t^k = (p_{t,x}^k, p_{t,y}^k)$ , velocity  $\mathbf{v}_t^k = (v_{t,x}^k, v_{t,y}^k)$ , and acceleration  $\mathbf{a}_t^k = (a_{t,x}^k, a_{t,y}^k)$ . Here, the velocity and acceleration are calculated from the position values by the following approximations:

$$\mathbf{v}_t^k \approx \frac{\mathbf{p}_t^k - \mathbf{p}_{t-1}^k}{\Delta t}, \quad \mathbf{a}_t^k \approx \frac{\mathbf{v}_{t+1}^k - \mathbf{v}_t^k}{\Delta t} \quad (1)$$

where  $\Delta t$  is the difference between adjacent time steps.

In our scenario, each  $\mathbf{x}_{1:T}^k$  has missing parts identified by a masking sequence  $\mathbf{m}_{1:T}^k = (m_1^k, \dots, m_T^k)$  where  $m_t^k = 1$  if  $\mathbf{x}_t^k$  is *observed* and 0 if it is *missing*. Then, an imputation model aims to take the incomplete data  $\{\mathbf{m}_{1:T}^k \odot \mathbf{x}_{1:T}^k\}_{k=1}^K$  as input and produce imputed trajectories  $\{\hat{\mathbf{x}}_{1:T}^k\}_{k=1}^K$ . Combining these with the observed fragments results in complete trajectories, i.e.,

$$\tilde{\mathbf{x}}_{1:T}^k = \mathbf{m}_{1:T}^k \odot \mathbf{x}_{1:T}^k + (\mathbb{1}_T - \mathbf{m}_{1:T}^k) \odot \hat{\mathbf{x}}_{1:T}^k, \quad k = 1, \dots, K. \quad (2)$$

The novelty of the proposed framework lies in the mechanism of enhancing the model performance by combining positions directly predicted by a neural network and those resulting from accumulating predicted derivatives (i.e., velocity and acceleration values). To elaborate on the details of the proposed mechanism, the remainder of this section consists of the following four parts: Section 3.1 describes the neural network for initial prediction, Section 3.2 introduces the derivative accumulation process for alternative predictions, Section 3.3 describes the weighted ensemble mechanism to combine multiple predictions resulting from the previous sections, and Section 3.4 explains the loss function for model training. See Fig. 2 illustrating the overall architecture of our framework.

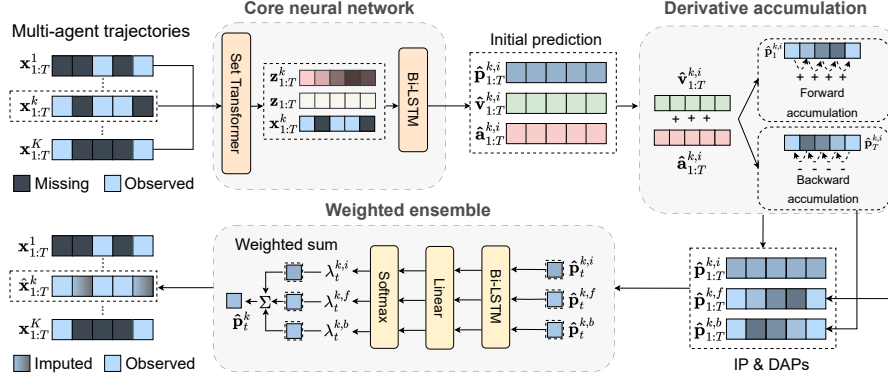


Fig. 2: Overview of the proposed framework.

### 3.1 Neural Network-Based Initial Prediction

This section describes the neural network architecture that makes *initial prediction* (IP) of imputed trajectories. It takes partially observed trajectories  $\{\mathbf{m}_{1:T}^k \odot \mathbf{x}_{1:T}^k\}_{k=1}^K$  as an input and predicts each player  $k$ 's full trajectory

$$\hat{\mathbf{x}}_{1:T}^{k,i} = \{(\hat{p}_{t,x}^{k,i}, \hat{p}_{t,y}^{k,i}, \hat{v}_{t,x}^{k,i}, \hat{v}_{t,y}^{k,i}, \hat{a}_{t,x}^{k,i}, \hat{a}_{t,y}^{k,i})\}_{t=1}^T, \quad (3)$$

where the superscript  $i$  stands for “initial”.

Since there is generally no inherent order among players in team sports, modeling their movements requires to ensure *permutation-equivariance*. That is, permuting the input order should not affect each player's output, except for applying the same permutation in the output order. Following a recent study on the ball trajectory inference in team sports [10], we employ Set Transformer [12] to ensure the permutation-equivariance of outputs.

To be specific, we obtain permutation-equivariant player-wise embeddings  $\{\mathbf{z}_t^k\}_{k=1}^K$  from the encoder of a Set Transformer and a single permutation-invariant embedding  $\mathbf{z}_t$  from a full Set Transformer for each time step  $t$ :

$$\begin{aligned} (\mathbf{z}_t^1, \dots, \mathbf{z}_t^K) &= \text{ST-Encoder}(m_t^1 \mathbf{x}_t^1, \dots, m_t^K \mathbf{x}_t^K), \\ \mathbf{z}_t &= \text{SetTransformer}(m_t^1 \mathbf{x}_t^1, \dots, m_t^K \mathbf{x}_t^K). \end{aligned} \quad (4)$$

Frame-by-frame application of the Set Transformer to the input features yields embeddings  $\{(\mathbf{z}_t^1, \dots, \mathbf{z}_t^K, \mathbf{z}_t)\}_{t=1}^T$ . Then, bidirectional LSTMs [9] sharing weights across players extract the sequential information from the concatenated sequence  $\{(\mathbf{x}_t^k, \mathbf{z}_t^k, \mathbf{z}_t)\}_{t=1}^T$  per player  $k$  by updating joint hidden states:

$$\mathbf{h}_t^{k,f} = \text{LSTM}^f(\mathbf{x}_t^k, \mathbf{z}_t^k, \mathbf{z}_t; \mathbf{h}_{t-1}^{k,f}), \quad \mathbf{h}_t^{k,b} = \text{LSTM}^b(\mathbf{x}_t^k, \mathbf{z}_t^k, \mathbf{z}_t; \mathbf{h}_{t+1}^{k,b}) \quad (5)$$

Lastly, a fully-connected layer decodes the joint hidden state to output a prediction  $\hat{\mathbf{x}}_t^{k,i} = \text{FC}(\mathbf{h}_t^{k,f}, \mathbf{h}_t^{k,b})$  at each time  $t$ . In later sections, we combine it with alternative predictions to get a more accurate final prediction.

### 3.2 Derivative-Accumulating Prediction

In this section, we start from the fact that players' acceleration values highly vary over time since it is directly related to their stochastic intents. In contrast, velocities are more correlated across neighboring time steps, and positions exhibit even stronger autocorrelation than their derivatives. This implies that accurately predicting acceleration values can lead to more stable and accurate position estimates, provided the physical relationships in Eq. (1) are maintained. However, since the model introduced in Section 3.1 does not enforce these relationships in its outputs  $\{\mathbf{x}_{1:T}^{k,i}\}_{k=1}^K$ , accurate prediction of the derivatives does not necessarily lead to improved position accuracy.

Taking this into account, we make alternative *derivative-accumulating predictions* (DAP), which enforces the physical relationships in Eq. (1) for improved stability. Specifically, given a missing segment  $(t_s, t_e)$  for a player  $k$ , we recursively predict positions inside the segment by accumulating velocities and accelerations in either direction using the following equation derived from Eq. (1):

$$\mathbf{p}_{t+1}^k \approx \mathbf{p}_t^k + \mathbf{v}_{t+1}^k \Delta t, \quad \mathbf{v}_{t+1}^k \approx \mathbf{v}_t^k + \mathbf{a}_t^k \Delta t. \quad (6)$$

That is, along the forward direction, we start from the observed position  $\mathbf{p}_{t_s}^k$  by setting  $\hat{\mathbf{p}}_{t_s}^{k,f} = \mathbf{p}_{t_s}^k$  and recursively add predicted velocities and accelerations to obtain *forward predictions*  $\hat{\mathbf{p}}_t^{k,f}$  for  $t \in (t_s, t_e)$  as follows:

$$\hat{\mathbf{p}}_t^{k,f} \approx \hat{\mathbf{p}}_{t-1}^{k,f} + \hat{\mathbf{v}}_t^{k,i} \Delta t \approx \hat{\mathbf{p}}_{t-1}^{k,f} + (\hat{\mathbf{v}}_{t-1}^{k,i} + \hat{\mathbf{a}}_{t-1}^{k,i} \Delta t) \Delta t \quad (7)$$

Likewise, we start from the observed position  $\mathbf{p}_{t_e}^k$  at the opposite endpoint and recursively subtract the predicted derivatives to obtain *backward predictions*  $\hat{\mathbf{p}}_t^{k,b}$ .

Adopting DAPs instead of initial prediction carries several advantages. First, since the loss between these DAPs and the ground truth penalizes unstable predictions of the velocity and acceleration, minimizing it improves the smoothness of the predicted derivatives. Considering that existing position-oriented imputation models suffer from fluctuating trajectories, these smooth derivatives have a clear advantage in that they result in more plausible positional predictions. Furthermore, enforcing the relationships between the physical quantities imposes an additional inductive bias on the model, making it more data-efficient.

### 3.3 Weighted Ensemble of Multiple Predictions

Although DAP introduced in Section 3.2 has clear advantages over IP resulting from Section 3.1, it also has a potential drawback known as the *error compounding problem*. Because DAP only relies on the observation at an endpoint as an anchor and the predicted derivatives that are accumulated on the anchor, prediction errors tend to grow as the number of iterations in Eq. (7) (or its backward counterpart) increases. In contrast, IP is robust to this problem since it is less sensitive to estimates at certain time steps.

To balance this trade-off, we take a hybrid approach that combines the strengths of both IP and DAP. Rather than exclusively relying on one prediction,

it performs a soft voting ensemble by computing a weighted sum of three predictions, IP and forward/backward DAPs. These weights are dynamically learned through an additional player-wise Bi-LSTM, which adapts the contribution of each prediction at each time step.

More specifically, for each player  $k$  and time step  $t$ , we feed the three predictions  $\hat{\mathbf{x}}_t^{k,i}, \hat{\mathbf{p}}_t^{k,f}, \hat{\mathbf{p}}_t^{k,b}$  along with the context embeddings  $\mathbf{z}_t^k, \mathbf{z}_t$  from Eq. (4) into a Bi-LSTM that updates its hidden states:

$$\tilde{\mathbf{h}}_t^{k,f} = \text{LSTM}^f(\hat{\mathbf{x}}_t^{k,i}, \hat{\mathbf{p}}_t^{k,f}, \hat{\mathbf{p}}_t^{k,b}, \mathbf{z}_t^k, \mathbf{z}_t, \gamma_t; \tilde{\mathbf{h}}_{t-1}^{k,f}), \quad (8)$$

$$\tilde{\mathbf{h}}_t^{k,b} = \text{LSTM}^b(\hat{\mathbf{x}}_t^{k,i}, \hat{\mathbf{p}}_t^{k,f}, \hat{\mathbf{p}}_t^{k,b}, \mathbf{z}_t^k, \mathbf{z}_t, \gamma_t; \tilde{\mathbf{h}}_{t+1}^{k,b}). \quad (9)$$

where  $\gamma_t = \exp(-\max\{0, \mathbf{W}_\gamma \delta_t + \mathbf{b}_\gamma\})$  is the temporal decay factor introduced in BRITS [2], indicating the distance of  $t$  from observed endpoints. We define  $\delta_t = (t - t_s, t_e - t)$  to provide symmetric time gaps for weighting the bidirectional DAPs. Then, a fully-connected layer with a softmax activation returns

$$(\lambda_t^{k,i}, \lambda_t^{k,f}, \lambda_t^{k,b}) = \text{Softmax}(\text{FC}(\tilde{\mathbf{h}}_t^{k,f}, \tilde{\mathbf{h}}_t^{k,b})) \quad (10)$$

that add up to 1. Based on these weights, the model yields a final prediction

$$\hat{\mathbf{p}}_t^k = \lambda_t^{k,i} \hat{\mathbf{p}}_t^{k,i} + \lambda_t^{k,f} \hat{\mathbf{p}}_t^{k,f} + \lambda_t^{k,b} \hat{\mathbf{p}}_t^{k,b}. \quad (11)$$

Combining this final prediction with the observed fragments by Eq. (2) results in complete trajectories across the entire period:

$$\tilde{\mathbf{x}}_{1:T}^k = \mathbf{m}_{1:T}^k \odot \mathbf{x}_{1:T}^k + (\mathbb{1}_T - \mathbf{m}_{1:T}^k) \odot \hat{\mathbf{x}}_{1:T}^k, \quad (12)$$

where  $\hat{\mathbf{x}}_t^k = (\hat{p}_{t,x}^k, \hat{p}_{t,y}^k, \hat{v}_{t,x}^{k,i}, \hat{v}_{t,y}^{k,i}, \hat{a}_{t,x}^{k,i}, \hat{a}_{t,y}^{k,i})$ .

### 3.4 Loss Function

In our framework, improving the accuracy of the prediction at each stage contributes to a more reliable ensemble output. Therefore, we minimize not only the loss between the final ensemble prediction and the true trajectories but also the loss of each auxiliary prediction. Specifically, we compute the mean absolute errors (MAEs) for the IP and DAPs as well as the ensemble prediction, respectively, and train the entire architecture by minimizing the sum of these MAEs. Formally, for the MAE losses  $\mathcal{L}^i$  of the IP,  $\mathcal{L}^f$  and  $\mathcal{L}^b$  for the bidirectional DAPs, and  $\mathcal{L}^h$  for the ensemble prediction, the model is trained by minimizing

$$\mathcal{L}^{\text{MIDAS}} = \mathcal{L}^i + \mathcal{L}^f + \mathcal{L}^b + \mathcal{L}^h. \quad (13)$$

Table 1: Details on the Three Sports Datasets.

Split	Soccer		Basketball		American Football	
	Matches	Frames	Matches	Frames	Matches	Frames
<b>Train.</b>	2	70,119	70	1,843,329	-	425,000
<b>Valid.</b>	0.5	20,690	10	249,474	-	52,150
<b>Test</b>	0.5	21,424	20	529,764	-	-

## 4 Experiments

In this section, we conduct experiments on multiple sports datasets to evaluate the performance of MIDAS and its generalizability across different sports.

### 4.1 Data Preparation

In the experiments, we independently train and evaluate models on three public datasets collected from popular team sports: soccer, basketball, and American football. The soccer dataset is provided by Metrica Sports<sup>7</sup> and contains tracking data for 22 players collected across three matches. For basketball, we use 100 matches among 631 matches of SportsVU NBA dataset<sup>8</sup>, which includes trajectories of 10 players per match. The American football dataset is from the Kaggle competition<sup>9</sup> based on NFL’s Next Gen Stats. We adopt its preprocessed version<sup>10</sup> provided by NRTSI paper [20], which contains 9,543 five-second time series of six offensive players. The original sampling rates of the three datasets are 25Hz, 25Hz, and 10Hz, respectively, but we downsample all datasets to 10Hz for consistency. As model inputs, we use 200 frames (20 seconds) per sequence for soccer and basketball and 50 frames (5 seconds) for American football.

### 4.2 Missing Scenarios

To evaluate the model performance on various missing patterns, we consider the following three scenarios that may occur during data acquisition processes:

1. Uniform missing: All players have missing values at the same time interval. Note that among the baselines, NAOMI [15] and NRTSI [20] are designed to only handle this scenario and are not capable of the following other scenarios.
2. Agent-wise missing: Individual players have different missing intervals.
3. Broadcasting camera: A virtual camera follows the ball and only captures the players inside the camera view, resulting in missing values for the remaining players as shown in Fig. 1. Following Graph Imputer [18], we conduct experiments only on the soccer dataset for this scenario.

<sup>7</sup> <https://github.com/metrica-sports/sample-data>

<sup>8</sup> <https://github.com/linouk23/NBA-Player-Movements>

<sup>9</sup> <https://www.kaggle.com/competitions/nfl-big-data-bowl-2021>

<sup>10</sup> [https://github.com/lupalab/NRTSI/tree/main/codes\\_stochastic](https://github.com/lupalab/NRTSI/tree/main/codes_stochastic)



Fig. 3 illustrates examples of masking matrices from the soccer dataset used in each missing scenario. Since our task is to impute trajectories given observed data before and after the missing intervals, we ensure that the first and last five frames of each sequence are always observable, following previous work [15,18,20]. During training, we apply a dynamic missing rate ranging from 0.1 to 0.9, while testing is conducted with a fixed missing rate of 0.5 to encourage the model to generalize across various missing rate scenarios. Additional evaluations with different missing rates are presented as an the ablation study in Section 4.5.



Fig. 3: Visualization of example masking matrices for three different missing scenarios.

### 4.3 Baseline Models and Evaluation Metrics

In the experiments, we compare the imputation performance of MIDAS with several baselines, including naive methods such as linear interpolation (LI) and cubic spline (CS), as well as deep learning models such as BRITS [2], NAOMI [15], NRTSI [20], CSDI [23], Graph Imputer (GI) [18], and ImputeFormer (IF) [17]. To evaluate the impact of our derivative-accumulating self-ensemble mechanism, we also implement a baseline that only uses the initial prediction (IP) described in Section 3.1 and is trained with the loss  $\mathcal{L}^i$  from Section 3.4. For models such as BRITS, NAOMI, and CSDI that do not preserve permutation-equivariance of input players, we sort trajectories by the sum of their average  $x$  and  $y$  coordinates to ensure permutation robustness. We compare these baselines using two evaluation metrics: (1) *position error* (PE) indicating the average Euclidean distance between the true and predicted positions and (2) *step change error* (SCE) [15,20] defined as the average absolute difference between the variance of the true and predicted velocities to assess the trajectories’ physical plausibility.

### 4.4 Main Experimental Results

The resulting Table 2 shows that the proposed MIDAS consistently outperforms other baselines in both positional accuracy (PE) and physical plausibility (SCE). Linear interpolation (LI) and cubic spline (CS) offer simple yet competitive results in some scenarios. Notably, deep learning baselines such as BRITS, NAOMI, and CSDI, which are not designed for multi-agent domains, often fail to exceed these naive baselines. Similarly, Graph Imputer (GI) performs worse than LI and CS in many cases despite its dedicated architecture for sports contexts, as previously reported in its original article [18].

By contrast, our model for initial prediction (IP) already surpasses most baselines, demonstrating its strength in modeling dynamic multi-agent interactions. Furthermore, comparing IP and MIDAS highlights the effectiveness of our self-ensemble mechanism. By effectively leveraging the complementary

Table 2: Performance of imputation models on different datasets and scenarios.

Scenario	Metric	Method									
		LI	CS	BRITS	NAOMI	NRTSI	CSDI	GI	IF	IP	MIDAS
Soccer											
Uniform	PE	3.8406	2.2085	7.4859	4.5343	3.1791	3.4295	4.6511	2.0898	1.4563	<b>1.3205</b>
	SCE	0.1299	0.0867	3.9089	3.9793	0.0854	0.1586	0.1191	0.0815	0.1488	<b>0.0516</b>
Agent-wise	PE	5.0752	11.4647	5.7266	—	—	4.0279	5.6011	2.5798	2.0755	<b>1.9832</b>
	SCE	0.1631	0.2939	2.9627	—	—	0.1305	0.1508	0.0976	0.1057	<b>0.0535</b>
Camera	PE	3.1083	1.9209	7.4208	—	—	3.5181	3.6512	2.2151	1.4879	<b>1.2296</b>
	SCE	0.0993	0.0547	4.1967	—	—	0.2132	0.0934	0.3149	0.1554	<b>0.0374</b>
Basketball											
Uniform	PE	3.3481	2.3114	2.9085	1.5254	2.5291	2.2558	2.8305	1.3622	0.9801	<b>0.9727</b>
	SCE	0.1483	0.1025	1.0521	0.3230	0.0734	0.0631	0.1066	0.0531	<b>0.0432</b>	0.0438
Agent-wise	PE	4.4992	10.3857	2.4238	—	—	2.3471	2.5859	<b>1.3345</b>	1.3832	1.3862
	SCE	0.1787	0.2715	0.5397	—	—	0.0563	0.0700	0.0485	<b>0.0373</b>	0.0381
American Football											
Uniform	PE	0.8897	0.7448	1.7990	0.9692	0.5158	0.5558	0.8899	0.3673	0.2073	<b>0.1542</b>
	SCE	1.1063	0.9463	10.9459	2.3112	0.2989	0.4905	1.1023	0.2858	0.1990	<b>0.1126</b>
Agent-wise	PE	1.5128	1.2041	1.7527	—	—	0.6182	1.5128	0.3944	0.2383	<b>0.2104</b>
	SCE	1.0641	0.5306	10.6807	—	—	0.4288	1.0631	0.1869	0.1180	<b>0.0967</b>

strengths of initial predictions and alternative derivative-accumulating predictions, it leads to superior performance even compared to state-of-the-art methods such as ImputeFormer (IF) in most scenarios.

Such observations are also evident in Fig. 4, where LI, NRTSI, and CSDI often generate unrealistic trajectories, either overly linear or changing direction too frequently, resulting in erratic and implausible motion patterns. In contrast, IF and MIDAS produce trajectories that closely resemble true player movements, as indicated by the relatively low PEs over the missing interval.

Meanwhile, an interesting observation emerges in the basketball dataset, where IP and IF show performance comparable to or slightly better than MIDAS in some cases. We attribute this to the larger amount of training data available (70 games), which may reduce the relative advantage of MIDAS. In contrast, for soccer and American football, where training data are more limited, MIDAS’s derivative-based self-ensemble mechanism demonstrates its data efficiency by significantly outperforming other methods. This data efficiency is particularly important in real-world sports applications, where acquiring large amounts of complete tracking data is often difficult due to the competitive and commercial nature of professional sports.

#### 4.5 Ablation Studies

In addition to the main experiments, we carried out an ablation study to examine the impact of each component of MIDAS. We also conducted a comparative analysis on the performance of the framework under different sequence lengths

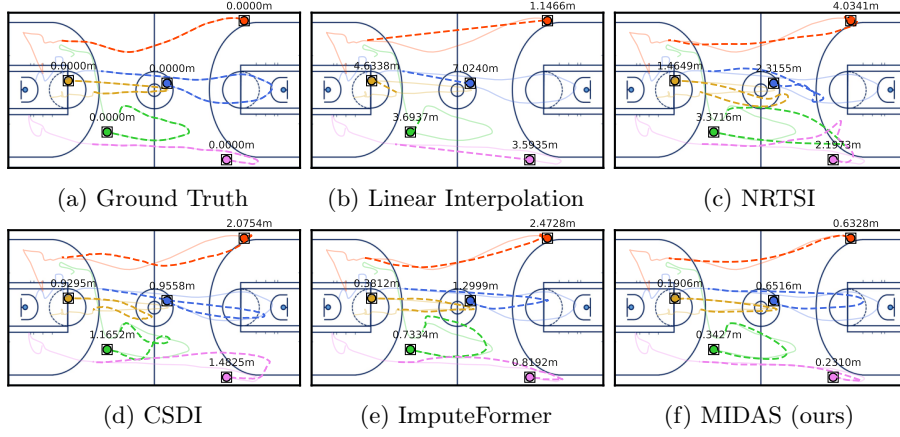


Fig. 4: Comparison of ground truth and imputed trajectories for the uniform missing scenario in basketball. The solid lines indicate the ground truth trajectories, while the dashed ones show imputed trajectories resulting from different methods. Circles indicate the players’ locations at the last frame, and the annotated values represent average position errors over the missing interval.

Table 3: Position errors of the components of MIDAS in Eq. (11) trained using different subsets of features.

IP Features	DAP Features	$\hat{\mathbf{p}}_t^{k,i}$	$\hat{\mathbf{p}}_t^{k,f}$	$\hat{\mathbf{p}}_t^{k,b}$	$\hat{\mathbf{p}}_t^k$
Position	Velocity	4.0008	2.8203	2.8261	2.5549
Position	Vel. & accel.	2.9119	2.6973	2.6858	2.4954
Pos. & vel.	Velocity	1.6600	1.5742	1.5590	1.4025
Pos. & vel.	Vel. & accel.	1.6235	1.5731	1.5670	1.4013
All features	Velocity	1.6713	1.4985	1.5595	1.2644
All features	Vel. & accel.	<b>1.4963</b>	<b>1.4122</b>	<b>1.3982</b>	<b>1.2296</b>

and missing rates. For simplicity, both experiments were conducted only on the broadcasting camera scenario in the soccer dataset.

*Impact of the Derivatives as Features* To empirically justify the use of derivative features in IP and DAP, we compared the performance of MIDAS on the broadcasting camera scenario with those trained without accelerations (i.e., using positions and velocities) and even without velocities (i.e., only using positions) of observed trajectories. Furthermore, we configured IP predict only positions and velocities, and DAP estimate positions only based on predicted velocities. We then compared these “velocity-only” DAP models with their counterparts that also incorporate predicted accelerations as in Eq. (7).

As shown Table 3, providing velocities and accelerations as input features for IP clearly improves the imputation performance. We attribute this to the

Table 4: Position errors of the MIDAS trained for and applied to scenarios with different sequence lengths and missing rates. We report the missing rate of the camera scenario alongside since it varies according to the sequence length.

SL \ MR	0.3	0.5	0.7	Camera (MR)
<b>50</b>	0.0691	0.1158	0.1552	0.0841 (0.4569)
<b>100</b>	0.3561	0.5948	0.8047	0.4622 (0.5138)
<b>200</b>	1.2805	2.0491	2.5556	1.2296 (0.5375)
<b>300</b>	2.3129	3.2746	4.0821	1.5993 (0.5454)
<b>600</b>	4.2597	5.9329	7.2485	2.1410 (0.5540)

neural network architecture for IP, where Set Transformers independently encode multi-agent contexts at each time step via Set Transformers, and player-wise Bi-LSTMs link temporal information. Providing derivatives as input allows the Set Transformers to utilize information of adjoining time steps, resulting in more comprehensive context embeddings compared to using positions alone.

In addition, we observe consistent performance improvements when predicted accelerations are incorporated into DAP alongside velocities (i.e., rows 2, 4, and 6 versus 1, 3, and 5, respectively). We attribute this to the fact that including accelerations enables DAP to capture the finer dynamics of player motion, mitigating the drift caused by error compounding in velocity-only DAP.

*Results on Different Sequence Lengths and Missing Rates* In addition, we compare the model’s performance under different sequence lengths and missing rates. Agreeing with our intuition, Table 4 shows that the model becomes less accurate as either the sequence length or the missing rate increases. In particular, the position error of the agent-wise missing scenario becomes much larger for a longer sequence, even with a small missing rate. This is because some players may miss most frames in the process of randomly distributing the total number of missing frames to individuals. Accordingly, in a longer sequence, the model has to predict the players’ stochastic movements for tens of seconds, resulting in a large error due to its inherent difficulty. Meanwhile, in the broadcasting camera scenario, the maximum length of a missing segment does not significantly change according to the sequence length. This results in robust performance against varying sequence lengths, implying that our framework can be reliably applied to real-world broadcasting data.

#### 4.6 Computational Complexity Analysis

In this section, we analyze the computational complexity of MIDAS. The analysis considers three key parameters: the number of time steps  $T$ , the hidden dimension  $m$ , and the number of players  $K$ . It takes  $O(TK^2m)$  for Set Transformer used in the initial prediction,  $O(TKm^2)$  for Bi-LSTMs employed in the initial prediction and weighted ensemble. In total,  $O(TK^2m + TKm^2) \approx O(TKm^2)$  as  $m \gg K$ .

Since Bi-LSTM adopts a recurrent structure, the entire computation process proceeds over  $O(T)$  steps, proportional to the length of the sequence.

## 5 Applications

In Section 4, we evaluate model performance primarily based on metrics related to missing periods in sports data. In practice, however, what is more important in this domain is the quality of the trajectories for the entire period, as they can be utilized in diverse domain-specific downstream tasks. As examples, we present two promising applications in the soccer domain: approximating physical statistics and pass success probability from incomplete tracking data.

### 5.1 Approximation of Physical Statistics for Load Management

In this section, we explore how accurately our method can estimate statistics for a given period when imputed trajectories are combined with known observations. Specifically, we compare the *total distance* covered by a player and the *number of sprints* estimated by each method, as they are widely used as indicators for players’ physical performance or fitness. We first compute velocities from the observed/imputed positions based on Eq. 1 and obtain speed values by calculating the norms of these velocity vectors. To make the best estimation from given positional predictions, we remove outliers whose speed is larger  $12\text{ m s}^{-1}$  or whose norm of the acceleration exceeds  $8\text{ m s}^{-2}$  and replace the values by linear interpolation. Also, we smoothen the resulting speed signal by applying a Savitzky-Golay filter [19]. After preprocessing speed signals, we compute the distance covered by each player by summing the speed values multiplied by  $\Delta t = 0.1\text{s}$ . For the latter, if a player runs faster than  $6\text{ m s}^{-1}$  for consecutive frames, we detect his/her movement during the frames as *sprint* and count the number of such sprints the player made during the given period.

Table 5: Players’ physical statistics estimated by different models and their mean absolute percentage errors (MAPE) for the soccer test data.

Method	Distance (m)		Sprint Count	
	Mean	MAPE	Mean	MAPE
Ground Truth	11,093.5	—	41.49	—
Linear Interpolation	10,167.8	8.46%	38.89	6.32%
Cubic Spline	10,686.3	3.73%	38.85	6.73%
BRITS	10,979.2	2.76%	59.89	53.62%
CSDI	11,343.0	2.77%	44.20	14.71%
Graph Imputer	8,972.1	19.15%	37.85	9.80%
ImputeFormer	11,441.7	3.22%	50.25	26.29%
MIDAS (ours)	<b>10,922.4</b>	<b>1.58%</b>	<b>40.71</b>	<b>4.95%</b>

For evaluation, we use the soccer test data consisting of the half of a match and assume the broadcasting camera scenario. Since players played for different time periods, we normalize each player’s statistics by 90 minutes and calculate the averages of such normalized values estimated by MIDAS and other baselines, respectively. Note that players who ran fewer than two sprints during the half were excluded from every evaluation.

According to Table 5, MIDAS provides accurate estimates close to the ground truth. Especially considering that almost all baselines either suffer from inaccurate distance measures (linear interpolation, cubic spline, and Graph Imputer) or overestimate speed spikes (BRITS, CSDI, and ImputeFormer), it is obvious that our model takes clear advantage of smooth prediction of velocities. In a nutshell, our framework is practical in that it can provide reliable statistics with incomplete tracking data, which originally require complete player trajectories.

## 5.2 Approximation of Pass Success Probability for Spatial Analysis

One representative example of leveraging player tracking data for match analysis is Pitch Control [21], which estimates the probability that a pass to each location on the pitch would be successful. Such pass success probabilities for different

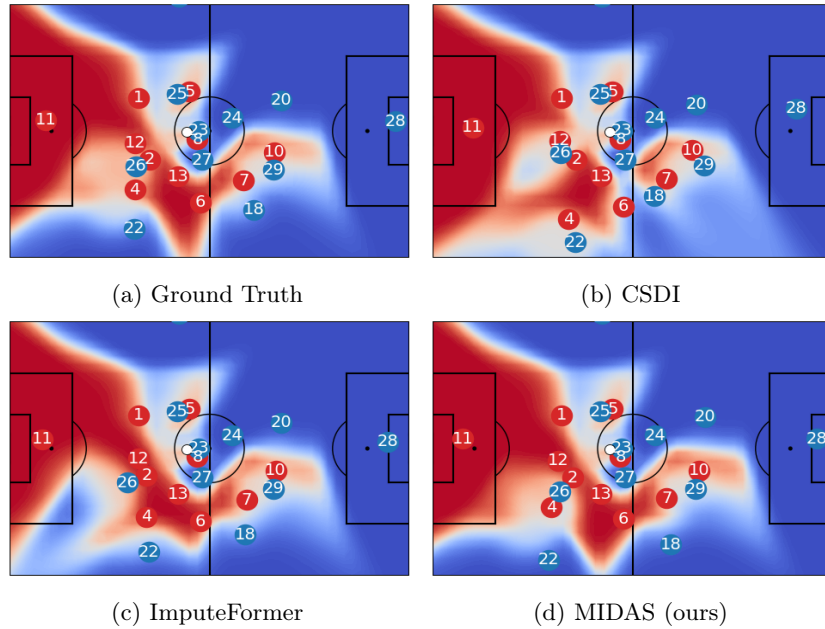


Fig. 5: Pass success probability maps based on true and imputed player positions resulting from different methods in a partially-observable camera setting. Darker red and blue regions indicate a higher probability of the left and right teams gaining possession, respectively, if the ball is passed to those areas.

destinations are typically visualized as a heat map overlayed on the pitch, so that domain experts can evaluate players’ positioning and decision-making for both actual and hypothetical passes to different locations on the pitch.

Thus, to demonstrate the applicability of imputation models in actual match analysis, we compare the Pitch Control maps generated using the player positions imputed by different methods. In the situation in Fig. 5 as an example, player 23 of the blue team has the ball, while his teammates 22 and 26 are making forward runs towards the open spaces on the left flank and in the center behind the red defensive line, respectively. The ground truth map (Fig. 5(a)) indicates that the blue team has a slightly higher control probability in both areas, reflecting reasonable pass success opportunities to these players, who are onside. However, inaccurate imputations by CSDI (Fig. 5(b)) and ImputeFormer (Fig. 5(c)) lead to issues such as players being mispredicted in offside positions or pass success probabilities being over- or underestimated in critical areas. In contrast, MIDAS (Fig. 5(d)) produces predictions that closely follow the actual player dynamics, resulting in probability maps that more accurately reflect the true game situation. This example instantiates how our framework facilitates more reliable downstream analysis by providing accurate imputation results.

## 6 Conclusions

This paper proposes MIDAS, a framework for imputing missing values in multi-agent trajectories with high accuracy and physical plausibility. MIDAS combines a permutation-equivariant neural network for initial trajectory prediction with a self-ensemble mechanism that incorporates derivative-based alternative predictions to refine imputation results and enforce physical consistency. Experiments on three team sports datasets under various missing scenarios demonstrate the effectiveness of our approach in generating trajectories with higher positional accuracy and improved reality than existing baselines. While this study focuses on team sports, we believe the proposed framework is applicable to other spatiotemporal domains. Future work will explore extending MIDAS to additional domains such as autonomous driving and crowd simulation, as well as its application to downstream tasks that require complete and reliable trajectory data.

## References

1. Battaglia, P.W., Hamrick, J.B., Bapst, V., Sanchez-Gonzalez, A., Zambaldi, V.F., Malinowski, M., Tacchetti, A., Raposo, D., Santoro, A., Faulkner, R., Gülçehre, Ç., Song, H.F., Ballard, A.J., Gilmer, J., Dahl, G.E., Vaswani, A., Allen, K.R., Nash, C., Langston, V., Dyer, C., Heess, N., Wierstra, D., Kohli, P., Botvinick, M.M., Vinyals, O., Li, Y., Pascanu, R.: Relational inductive biases, deep learning, and graph networks. CoRR **abs/1806.01261** (2018), <http://arxiv.org/abs/1806.01261>
2. Cao, W., Wang, D., Li, J., Zhou, H., Li, L., Li, Y.: BRITS: Bidirectional recurrent imputation for time series. In: Advances in Neural Information Processing Systems 31 (2018)

3. Capellera, G., Ferraz, L., Rubio, A., Agudo, A., Moreno-Noguer, F.: TranSPORTmer: A holistic approach to trajectory understanding in multi-agent sports. In: Proceedings of the 17th Asian Conference on Computer Vision (2024)
4. Che, Z., Purushotham, S., Cho, K., Sontag, D.A., Liu, Y.: Recurrent neural networks for multivariate time series with missing values. *Scientific Reports* **8** (2018)
5. Choi, M., Lee, C.: Conditional information bottleneck approach for time series imputation. In: Proceedings of the 12th International Conference on Learning Representations (2023)
6. Cini, A., Marisca, I., Alippi, C.: Filling the g\_ap\_s: Multivariate time series imputation by graph neural networks. In: Proceedings of the 10th International Conference on Learning Representations (2022)
7. Du, W., Côté, D., Liu, Y.: SAITS: Self-attention-based imputation for time series. *Expert Systems with Applications* **219** (2023)
8. Gupta, A., Johnson, J., Fei-Fei, L., Savarese, S., Alahi, A.: Social GAN: Socially acceptable trajectories with Generative Adversarial Networks. In: IEEE Conference on Computer Vision and Pattern Recognition (2018)
9. Hochreiter, S., Schmidhuber, J.: Long short-term memory. *Neural Computation* **9**(8), 1735–1780 (1997)
10. Kim, H., Choi, H., Kim, C.J., Yoon, J., Ko, S.: Ball trajectory inference from multi-agent sports contexts using set transformer and hierarchical bi-lstm. In: Proceedings of the 29th ACM SIGKDD Conference on Knowledge Discovery and Data Mining (2023)
11. Kipf, T.N., Fetaya, E., Wang, K., Welling, M., Zemel, R.S.: Neural relational inference for interacting systems. In: Proceedings of the 35th International Conference on Machine Learning (2018)
12. Lee, J., Lee, Y., Kim, J., Kosiorek, A.R., Choi, S., Teh, Y.W.: Set Transformer: A framework for attention-based permutation-invariant neural networks. In: Proceedings of the 36th International Conference on Machine Learning (2019)
13. Li, J., Yang, F., Tomizuka, M., Choi, C.: EvolveGraph: Multi-agent trajectory prediction with dynamic relational reasoning. In: *Advances in Neural Information Processing Systems* 33 (2020)
14. Liu, S., Li, X., Cong, G., Chen, Y., Jiang, Y.: Multivariate time-series imputation with disentangled temporal representations. In: The 11th International Conference on Learning Representations (2023)
15. Liu, Y., Yu, R., Zheng, S., Zhan, E., Yue, Y.: NAOMI: non-autoregressive multi-resolution sequence imputation. In: *Advances in Neural Information Processing Systems* 32 (2019)
16. Marisca, I., Cini, A., Alippi, C.: Learning to reconstruct missing data from spatiotemporal graphs with sparse observations. In: *Advances in Neural Information Processing Systems* 35 (2022)
17. Nie, T., Qin, G., Ma, W., Mei, Y., Sun, J.: ImputeFormer: Low rankness-induced transformers for generalizable spatiotemporal imputation. In: Proceedings of the 30th ACM SIGKDD Conference on Knowledge Discovery and Data Mining (2024)
18. Omidshafiei, S., Hennes, D., Garnelo, M., Wang, Z., Recasens, A., Tarassov, E., Yang, Y., Elie, R., Connor, J., Muller, P., Mackraz, N., Cao, K., Moreno, P., Sprechmann, P., Hassabis, D., Graham, I., Spearman, W., Heess, N., Tuyls, K.: Multiagent off-screen behavior prediction in football. *Scientific Reports* **12** (2022)
19. Savitzky, A., Golay, M.J.E.: Smoothing and differentiation of data by simplified least squares procedures. *Analytical Chemistry* **36**(8) (1964)
20. Shan, S., Li, Y., Oliva, J.B.: NRTSI: Non-recurrent time series imputation. In: IEEE International Conference on Acoustics, Speech and Signal Processing (2023)



21. Spearman, W., Basye, A., Dick, G., Hotovy, R., Pop, P.: Physics-based modeling of pass probabilities in soccer. In: MIT Sloan Sports Analytics Conference (2017)
22. Sun, F., Kauvar, I., Zhang, R., Li, J., Kochenderfer, M.J., Wu, J., Haber, N.: Interaction modeling with multiplex attention. In: Advances in Neural Information Processing Systems 35 (2022)
23. Tashiro, Y., Song, J., Song, Y., Ermon, S.: CSDI: Conditional score-based diffusion models for probabilistic time series imputation. In: Advances in Neural Information Processing Systems 34 (2021)
24. Wu, H., Hu, T., Liu, Y., Zhou, H., Wang, J., Long, M.: TimesNet: Temporal 2D-variation modeling for general time series analysis. In: Proceedings of the 11th International Conference on Learning Representations (2023)
25. Yeh, R.A., Schwing, A.G., Huang, J., Murphy, K.: Diverse generation for multi-agent sports games. In: IEEE/CVF Conference on Computer Vision and Pattern Recognition (2019)
26. Yoon, J., Zame, W.R., van der Schaar, M.: Estimating missing data in temporal data streams using multi-directional recurrent neural networks. *IEEE Transactions on Biomedical Engineering* **66**(5), 1477–1490 (2019)
27. Yuan, Y., Weng, X., Ou, Y., Kitani, K.: AgentFormer: Agent-aware transformers for socio-temporal multi-agent forecasting. In: IEEE/CVF International Conference on Computer Vision (2021)